International Journal of Mass Spectrometry 407 (2016) 118–125

Contents lists available at ScienceDirect

International Journal of Mass Spectrometry

journal homepage: www.elsevier.com/locate/ijms

Photodissociation and density functional calculations of A_2M^+ and G_2M^+ (A = adenine, G = guanine, M = Cu, Ag, and Au) cluster ions

Guo-Jin Cao [a], Hong-Guang Xu [b,c], Xi-Ling Xu [b,c], Peng Wang [b,c], Wei-Jun Zheng [b,c,*]

[a] Institute of Molecular Science, Shanxi University, Taiyuan 030006, China
[b] Beijing National Laboratory for Molecular Sciences, State Key Laboratory of Molecular Reaction Dynamics, Institute of Chemistry, Chinese Academy of Sciences, Beijing 100190, China
[c] University of Chinese Academy of Sciences, Beijing 100049, China

ARTICLE INFO

Article history:
Received 11 June 2016
Received in revised form 17 July 2016
Accepted 20 July 2016
Available online 22 July 2016

Keywords:
Photodissociation
Density functional calculations
Nucleobases
Cluster cations

ABSTRACT

To understand the interactions between nucleobases and coinage metal cations, we conducted combined photodissociation and density functional theory studies on A_2M^+ and G_2M^+ (A = adenine, G = guanine, M = Cu, Ag, and Au) cations. The nucleobase-metal complexes were produced by laser ablation and detected by a reflectron time-of-flight mass spectrometer. The mass peaks of A_2M^+ and G_2M^+ cations have high intensities in the mass spectra of A_nM^+ and G_nM^+ complexes, indicating that these cations have relatively high stabilities. They were mass-selected and then photodissociated by 266 nm photons. Their photodissociation spectra clearly show that the loss of adenine or guanine is the predominant channel for these complexes. The density functional theory calculations show that A_2M^+ and G_2M^+ complexes prefer planar structures with the metal cations interacting with the N atoms in the carbon-nitrogen rings of adenine and guanine. The calculated bond dissociation energies of different dissociation channels are in good agreement with the experimental observed fragment ions.

© 2016 Elsevier B.V. All rights reserved.

Contents

1. Introduction 118
2. Experimental and theoretical methods 119
3. Experimental results 119
4. Theoretical results and discussion 120
   4.1. A_2Cu^+, A_2Ag^+, and A_2Au^+ 122
   4.2. G_2Cu^+, G_2Ag^+, and G_2Au^+ 122
5. Conclusions 124
Acknowledgements 124
Appendix A. Supplementary data 124
References ..... ??

1. Introduction

It is well known that metal ions play important roles in the biological processes involving DNA [1–3]. The presence of metal ions may influence the structures and functions of DNA molecules [4–7]. The interactions of metal ions with DNA are able to neutralize the negative charges on the phosphate backbone and stabilize the double-helical structures [8–11]. On the other hand, metal ions, especially the transition metal ions, binding directly to the nucleobases can usually disrupt the hydrogen bonds in base pairs and destabilize the double helix of DNA [12]. Metal ions binding indirectly to the phosphate groups also influence the sugar conformation and consequently influence DNA synthesis and the replication process. Some metal ions, such as iron and copper ions have the ability to produce reactive oxygen species which can induce lipid peroxidation and DNA damage [13–15]. Furthermore, studies show that metal cations can trigger the tautomerization

* Corresponding author at: Beijing National Laboratory for Molecular Sciences, State Key Laboratory of Molecular Reaction Dynamics, Institute of Chemistry, Chinese Academy of Sciences, Beijing 100190, China.
E-mail address: zhengwj@iccas.ac.cn (W.-J. Zheng).

http://dx.doi.org/10.1016/j.ijms.2016.07.008
1387-3806/© 2016 Elsevier B.V. All rights reserved.

processes. When these processes are connected with mismatch in the base pairing, they are able to increase the probabilities of gene mutations [16–21]. Thus, the interactions between metal ions and nucleobases are crucial in both biochemistry and supramolecular chemistry [2,22].

Investigating nucleobase-metal complexes in the gas phase can help us understand their interactions independent of the biomolecule backbone and solvent effects [23]. Thus, there were many studies on the nucleobase-metal complexes by theoretical calculations [24–32]. It has been shown by theoretical calculations that transition metal can bind to two or more different sites of nucleobases because the d-orbitals of transition metal ions are partially filled and they can easily form free radicals [33]. The density functional theory (DFT) calculations by Martinez and coworkers [24] suggested that Ag^+ and Au^+ cations can bind to the O4 or O2/N3 atoms of uracil while Cu^+ cation binds to O4 or O2 atoms of uracil. Their studies also show that Cu^+ cation mainly binds to the N3 or O7 atoms of cytosine; O7 or O8 atoms of thymine; N10, N9, N7, or N3 atoms of adenine; and N9, N7, O11, or N3 atoms of guanine [25,34]. Leal et al. [35] carried out a theoretical study on the Ag-nucleobase and Au-nucleobase complexes with neutral, cationic, and anionic charge states. There were also many experimental studies although it is difficult to generate nucleobase-metal complexes in the gas phase due to the low thermal stability and low vapor pressure of the nucleobases [36]. Rodgers et al. [37] studied the kinetic energy dependence and the simple collision-induced dissociation processes of AM^+ cation with xenon (M = Sc^+, Ti^+, V^+, Cr^+, Mn^+, Fe^+, Co^+, Ni^+, Cu^+, and Zn^+) using ion beam mass spectrometry. Yang and coworkers [38,39] investigated uracil-Mg^+, thymine-Mg^+ and cytosine-Mg^+ complexes by photodissociation experiments. Rajabi et al. investigated the structures of adenine-alkali metal complexes by infrared multi-photon dissociation (IRMPD) experiments [40]. The structures of cationized guanine complexes with alkaline metals have been determined with the IRMPD experiments [41,42]. Bowen and coworkers measured the photoelectron spectra of copper-nucleoside anionic complexes and investigated their structures and properties [43]. Cao et al. [44,45] investigated the Au-nucleobase complexes with anion photoelectron spectroscopy and theoretical calculations. Recently, Gao et al. [46] studied the structures and properties of C_2M^+ (C = cytosine, M = Li, Na, K, Cu, and Ag) using infrared spectroscopy in combination with DFT calculations.

In this work, we apply mass spectrometry and mass-selected laser photodissociation techniques in the gas phase to understand the interactions of the coinage metal cations with nucleobases (guanine and adenine). Based on the combination of experimental results and theoretical calculations, the preferred binding sites of guanine or adenine and the possible dissociation pathways of $(nucleobase)_2M^+$ (nucleobase = adenine, guanine, M = Cu, Ag, Au) cations were discussed.

2. Experimental and theoretical methods

The experiment was conducted on a home-built reflectron time-of-flight mass spectrometer (RTOF-MS) which has been described elsewhere [47]. The nucleobase-metal complexes were produced by laser ablation of rotating and translating disk targets (diameter 13 mm) with the second harmonic (532 nm) of a nanosecond Nd:YAG laser (Continuum Surelite II-10). Each disk target was prepared by pressing a powder mixture of metal (Cu, Ag or Au) and nucleobase (adenine, Sigma-Aldrich, 99%, or guanine, Alfa Aesar, 98 +%) at a molar ratio of 1:2. Helium gas with a backing pressure of 5.5 atm was delivered through a pulsed valve (General Valve Series 9) into the laser ablation source to cool the formed nucleobase-metal complexes. The cations of nucleobase-metal complexes were skimmed and drifted into the extraction region of the reflectron time-of-flight mass spectrometer. For the photodissociation experiments, the ions of interest were mass selected by a mass gate and were decelerated by a decelerator. The selected ions were then photodissociated by the fourth harmonic (266 nm) of another Nd:YAG laser (Continuum Surelite II-10, ~10 mJ/pulse, 6 mm diameter). The parent ions and the fragment ions were then reaccelerated, reflected by the reflectron plates and detected by a microchannel plates (MCP) detector.

To investigate the structures and energetics of A_2M^+ and G_2M^+ (M = Cu, Ag or Au) cations, the geometric structures were fully optimized without any symmetry restriction using DFT computations with the GAUSSIAN 09 program [48]. Optimized minimum structures were verified with nonexistence of imaginary frequencies in the analyses of vibrational frequencies. The Becke 3-parameter-Lee-Yang-Parr (B3LYP) [49,50] density functional method with the 6–31 + +G(d,p) basis set was used for nucleobases. The ECP10MDF, ECP28MDF, ECP60MDF relativistic effective core potential (RECP) developed by the Stuttgart-Cologne groups were chosen for Cu, Ag and Au, respectively [51]. Gaussian type one-electron basis sets ECP10MDF_VDZ, ECP28MDF_VDZ, and ECP60MDF_VDZ for Cu, Ag and Au, respectively, were used [51,52]. It has been verified that the energetic order of tautomers of nucleobases are in good agreement with the experimental results when density-functional approaches (B3LYP) and 6–31 + +G(d,p) basis sets were used for the complete geometry optimizations of nucleobases [44,45,53]. The bond dissociation energies (BDEs) are calculated based on the differences between the total energy of the parent ion and the total energies of all the fragments. The corrections of zero-point energy (ZPE) were also included in calculating the relative energies. TD-DFT calculations [54] were carried out to evaluate the properties of the excited states of the A_2M^+ and G_2M^+ cations, where M = Cu, Ag, and Au.

3. Experimental results

The mass spectra of $(nucleobase)_nCu^+$, $(nucleobase)_nAg^+$, $(nucleobase)_nAu^+$ (nucleobase = adenine, guanine) cations are shown in Figs. 1, 2, and 3 , respectively. The mass peaks of A_nCu^+ (n = 1–3) and G_nCu^+ (n = 1–5) cations are observed in Fig. 1, those of A_nAg^+ (n = 1–5) and G_nAg^+ (n = 1–7) cations are observed in Fig. 2, and those of A_nAu^+ (n = 1–3) and G_nAu^+ (n = 1–6) are observed in Fig. 3. Interestingly, compared to adenine, guanine is able to form relatively larger complexes with the metal ions at similar source conditions. The mass peaks of A_2M^+ and G_2M^+ (M = Cu, Ag, Cu) cations are stronger than their neighbors in the same series (A_nM^+ and G_nM^+). In addition to the nucleobase-metal complexes, protonated adenine and guanine clusters, A_nH^+ and G_nH^+ cations, are also detected in these mass spectra. There are some other low-intensity mass peaks in the spectra probably owing to the dissociation of adenine or guanine sample in the laser ablation. Those low intensity mass peaks do not affect the analysis of the mass spectra and the successive photodissociation experiments.

Fig. 4 shows the photodissociation mass spectra of A_2M^+ and G_2M^+ (M = Cu, Ag or Au) cations at 266 nm. The downward mass peaks stand for the depleted parent cation abundance, while the upward mass peaks show the relative intensities of the fragment ions. The predominant AM^+ and A^+ fragment ions have been observed for the dissociation spectra of A_2M^+ (M = Cu, Ag or Au) cations. The Ag^+ or Au^+ fragment ions have been found in the photodissociation mass spectra of A_2M^+ (M = Ag or Au) cations, but the Cu^+ fragment ion has not been detected in the photodissociation mass spectrum of A_2Cu^+ cation. For M = Cu, Ag, the intensity of AM^+ fragment ion is much stronger than that of A^+ fragment ion. Inversely, for M = Au, the intensity of A^+ fragment ion is much stronger than that of AAu^+ fragment ion. In addition, the photodis-

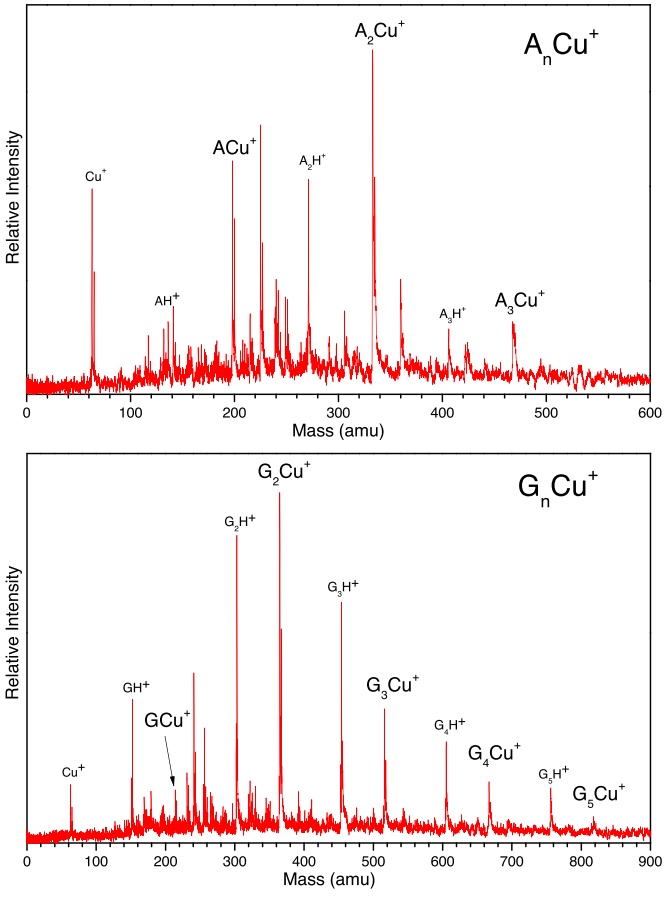

Fig. 1. Mass spectra of A_nCu^+ and G_nCu^+ cluster cations.

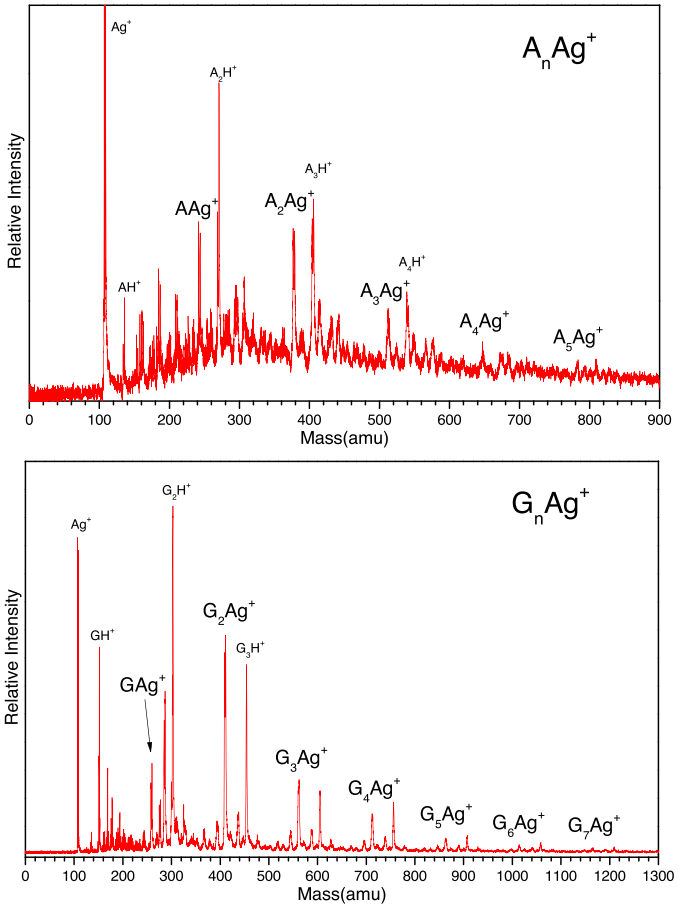

Fig. 2. Mass spectra of A_nAg^+ and G_nAg^+ cluster cations.

sociation of A_2Cu^+ cation produced a strong fragment mass peak centered at about 182 amu which may be associated to the formation of $(C_5N_4H_3)Cu^+$ cation upon loss NH_2 group from ACu^+ cation. A strong fragment mass peak centered at about 215 amu in the photodissociation spectrum of A_2Ag^+ cation may correspond to the formation of $(C_4N_4H_4)Ag^+$ cation due to the loss of HCN from AAg^+ cation, which is similar to the loss of HCN observed in electron ionization of nucleobases [55].

The products of GM^+ and G^+ fragment ions have been observed for the dissociation of G_2M^+ (M = Cu, Ag or Au) ions. Similar to the photodissociation of A_2Cu^+, the Cu^+ fragment ion has not been detected in the photodissociation of G_2Cu^+ cation. Also, the Au^+ fragment ion has not been observed in the photodissociation of G_2Au^+ cation at 266 nm. The photodissociation of both G_2Cu^+ and G_2Ag^+ cations produced a fragment ion mass peak centered at 178 amu probably due to the formation of $(C_6N_6H_6O)^+$. In addition, the photodissociation of G_2Cu^+ cation produced a strong fragment mass peak centered at about 198 amu which may be associated to the formation of $(C_5N_4H_3O)Cu^+$ cation upon loss NH_2 group from GCu^+ cation. A strong fragment mass peak centered at about 231 amu in the photodissociation spectrum of G_2Ag^+ cation may correspond to the formation of $(C_4N_4H_4O)Ag^+$ cation due to the loss of HCN from GAg^+ cation.

4. Theoretical results and discussion

In search of the global minimum of A_2M^+ and G_2M^+ (M = Cu, Ag or Au) cations, various possible initial geometric structures have been considered. Although IR spectra show that the amino-N9H tautomer is the only tautomer of adenine observed in low-temperature matrices [56], both amino-N7H and amino-N9H tautomers of adenine were recently observed in the IRMPD spectrum of electrosprayed protonated adenine dimer [57]. So in our calculations, A_2M^+ cations were investigated with amino-N7H and amino-N9H tautomers of adenine. With regard to the guanine monomer in gas phase, K-N7H, K-N9H, E-N7H, and E-N9H tautomers of guanine have been observed in the previous experiments [58–62]. Although the above-mentioned tautomers are considered in the former calculations, only the keto-keto guanine dimers were detected in the gas-phase IR-UV spectra [63,64]. Consequently, the K-N7H and K-N9H tautomers of guanine were taken into account in the search of low-energy isomers of G_2M^+ (M = Cu, Ag, Au) cations.

The low-energy isomers of these complexes are shown in Figs. 5 and 6. The optimized structures of $(nucleobase)_2M^+$ (nucleobase = adenine, guanine, M = Cu, Ag, Au) cations are in singlet spin states. The triplet and quintet spin states are much less stable. All of these complexes are planar structures in nucleobase-M^+-nucleobase style, containing a nearly linear N–M^+–N bond, similar to the structures of cytosine-M^+-cytosine (M = Cu or Ag)complexes [46,65]. That is in good agreement with the loss of nucleobase unit in all the dissociation experiments. Photodissociation fragment ions of these complexes detected at 266 nm are summarized in Table 1. The possible main dissociation channels and bond dissociation energies (BDEs) of the lowest-energy isomers of A_2M^+ and G_2M^+ cations are summarized in Table 2. Here, we only considered the lowest-energy isomers of A_2M^+ and G_2M^+ cations in the calculations of BDEs of possible photodissociation channels. Because the energy differences between the low-lying isomers of A_2M^+ cations are very small, their bond dissociation energies might be similar. Principal singlet–singlet and singlet–triplet electronic transitions, wavelengths and oscillator strengths (f) for the lowest-

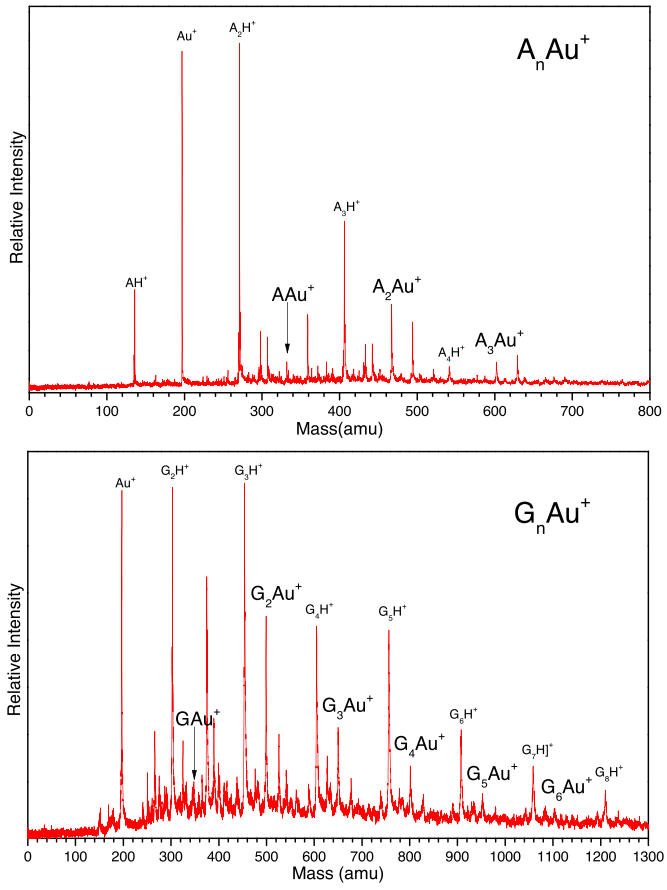

Fig. 3. Mass spectra of A_nAu^+ and G_nAu^+ cluster cations.

Table 1
Photodissociation fragment ions of A_2M^+ and G_2M^+ detected at 266 nm, where A = adenine ($C_5N_5H_5$), G = guanine ($C_5N_5H_5O$), M = Cu, Ag, and Au.

Parent ion	Fragment ions	
	m/z	photofragments
A_2Cu^+	135	A^+
	182	$(C_5N_4H_3)Cu^+$
	198	ACu^+
A_2Ag^+	107	Ag^+
	135	A^+
	215	$(C_4N_4H_4)Ag^+$
	242	AAg^+
A_2Au^+	135	A^+
	197	Au^+
	332	AAu^+
G_2Cu^+	151	G^+
	178	$(C_6N_6H_6O)^+$
	198	$(C_5N_4H_3O)Cu^+$
	214	GCu^+
G_2Ag^+	107	Ag^+
	151	G^+
	178	$(C_6N_6H_6O)^+$
	231	$(C_4N_4H_4O)Ag^+$
	258	GAg^+
G_2Au^+	151	G^+
	348	GAu^+

energy isomers of A_2M^+ and G_2M^+ cations, where M = Cu, Ag, and Au are summarized in Table S1. For A_2Cu^+ and G_2Cu^+ cations, the Cu d → A(N7) π and Cu d → G_2 π excitations can be classified as metal-to-ligand charge transfer (MLCT) processes, resulting in the formation of adenine or guanine cations, in good agreement with experimental results. For A_2Ag^+ cation, A(N9) π → Ag d excitation at 266 nm is able to be classified as ligand-to-metal charge transfer (LMCT) transitions, leading to the formation of Ag^+ cation.

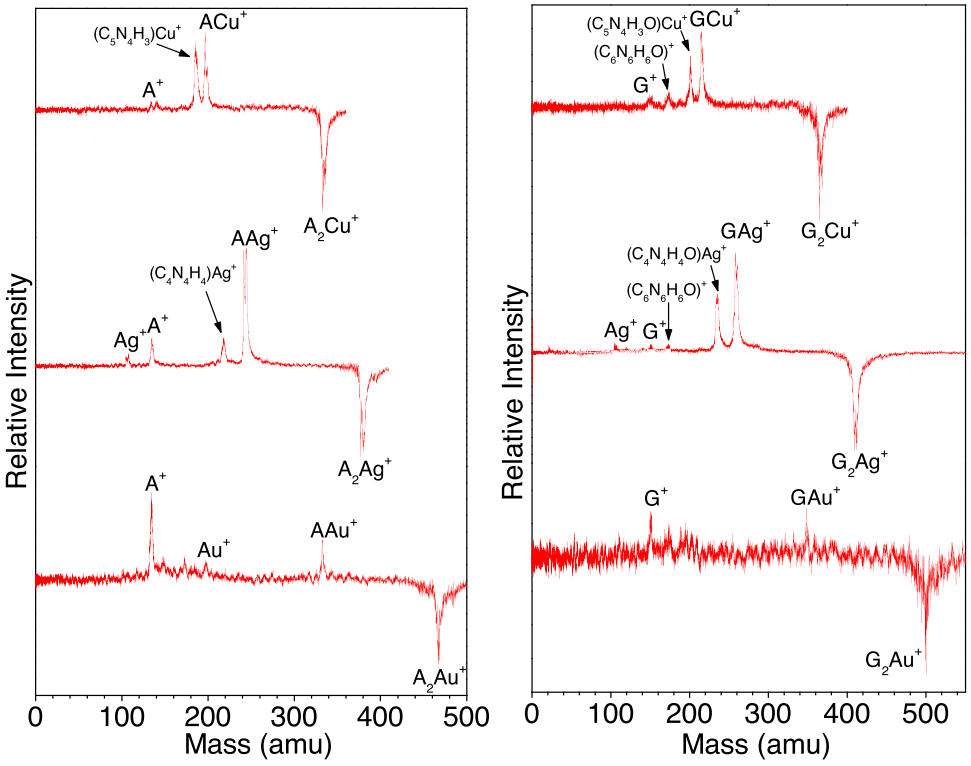

Fig. 4. Photodissociation mass spectra of the A_2M^+ and G_2M^+ cations at 266 nm, where M = Cu, Ag, and Au.

Table 2
The possible main dissociation channels and bond dissociation energies of the lowest-energy isomers of A_2M^+ and G_2M^+ cations, where M = Cu, Ag, and Au.

Dissociation channel	BDE (eV)		
	Cu	Ag	Au
(1a) $A_2M^+ \rightarrow A(N7)M^+ + A(N9)$	2.03	1.42	2.29
$A_2M^+ \rightarrow A(N9)M^+ + A(N7)$	2.65	2.06	2.77
(2a) $A_2M^+ \rightarrow A(N7)^+ + A(N9)M$	3.51	4.50	4.59
$A_2M^+ \rightarrow A(N9)^+ + A(N7)M$	3.31	4.30	4.39
(3a) $A_2M^+ \rightarrow A(N7)^+ + A(N9) + M$	5.66	4.40	4.65
$A_2M^+ \rightarrow A(N9)^+ + A(N7) + M$	5.46	4.20	4.45
(4a) $A_2M^+ \rightarrow M^+ + A_2$	4.89	3.56	3.50
(5a) $A_2M^+ \rightarrow M^+ + A(N7) + A(N9)$	5.21	3.88	5.79
(1g) $G_2M^+ \rightarrow GM^+ + G$	2.15	1.63	2.62
(2g) $G_2M^+ \rightarrow GM + G^+$	5.20	4.28	4.27
(3g) $G_2M^+ \rightarrow G + G^+ + M$	5.46	4.17	4.26
(4g) $G_2M^+ \rightarrow M^+ + G_2$	5.33	4.03	5.79
(5g) $G_2M^+ \rightarrow M^+ + G + G$	5.58	4.28	6.04

The photodissociation of A_2Ag^+ cation contains A(N9) $\pi \rightarrow$ A(N7) π intraligand (LL) charge transfer transition. G_2Ag^+ cation is firstly excited at 262 nm, higher than the photon energy of a 266 nm photon, indicating that the photodissociation might be a two-photon process.

4.1. A_2Cu^+, A_2Ag^+, and A_2Au^+

As can be seen in Fig. 5, the lowest-energy structure of A_2Cu^+ cation (isomer 1A) consists of amino-N7H and amino-N9H tautomers of adenine, which are both bound to Cu^+ cation through N3. The second lowest-energy isomer 1B has different proton donor group from the isomer 1A in the formation of N—H···N hydrogen bond. It lies only 1.5 kJ mol^{-1} above isomer 1A in energy. Both isomers 1A and 1B have planar structure with C_s symmetry.

As can be seen in Table 2, the BDEs of channels (1a) and (2a) of A_2Cu^+ cation are calculated to be 2.03 (or 2.65) and 3.51 (or 3.31) eV at the DFT/B3LYP level, respectively, much lower than the photon energy of a 266 nm photon (4.66 eV). The BDEs of channels (3a), (4a), and (5a) are calculated to be 5.66 (or 5.46), 4.89 and 5.21 eV, respectively, much higher than the photon energy of a 266 nm photon. Therefore, the most probable dissociation channel of A_2Cu^+ cation is by loss of adenine (N9) or adenine (N7) to produce ACu^+ cation (channel 1a) or adenine cation (channel 2a). That is in reasonable agreement with the observation of ACu^+ (channel 1a) and A^+ (channel 2a) fragment ions in the experiment (Fig. 4). The generation of Cu^+ fragment ion (channel 4a) requires 4.89 eV, which is higher than the photon energy of a 266 nm photon, indicating that at least two 266 nm photons are needed in order to generate Cu^+ fragment ion. That explains why Cu^+ fragment ion is not observed in our experiment. The BDEs of the loss of NH_2 group from $A(N7)Cu^+$ and $A(N9)Cu^+$ cations are 4.75 and 4.51 eV, respectively. So the loss of NH_2 group from $A(N9)Cu^+$ cation induced by another photon may be responsible for the formation of fragment peak centered at m/z = 182.

The most stable structure of A_2Ag^+ cation is isomer 2A but isomers 2B and 2C are higher than isomer 2A by only 0.3 and 0.6 kJ mol^{-1}, respectively. These three isomers are nearly degenerate in energy. The structure of isomer 2A is composed of amino-N7H and amino-N9H tautomers of adenine, which are bound to silver ion through N3 and N1, respectively. Besides, the N—H···N hydrogen bond is formed in isomer 2A. Isomer 2B with C_{2h} symmetry is consisted of two amino-N7H tautomers of adenine, which are both bound to silver ion through N3. We also note that hydrogen bond is not observed in isomer 2B. Both isomers 2A and 2C have planar structures with C_s symmetry. Because the energy differences between isomers 2D–2H and the most stable isomer (2A) are within 9.5 kJ mol^{-1}, we suspect that isomers 2D–2H might also exist in our experiments.

All the BDEs of channels (1a)–(5a) of A_2Ag^+ cation are lower than the photon energy of a 266 nm photon, indicating that all the channels (1a)–(5a) for A_2Ag^+ cation are possible photodissociation channels at 266 nm. Channel (1a) is the most probable channel. That explains why the Ag^+, A^+, and AAg^+ fragment ions are all observed in the photodissociation of A_2Ag^+ in our experiments. The BDEs of the simultaneous cleavage of N1-C2 and N3-C4 bonds of $A(N9)Ag^+$ and $A(N7)Ag^+$ cations are 4.51 and 4.53 eV, respectively, lower than the energy of a 266 nm photon. The fragment ion mass peak corresponding to $(C_4H_4N_4)Ag^+$ cation probably comes from the cleavages of N1-C2 and N3-C4 bonds of $A(N9)Ag^+$ and $A(N7)Ag^+$ cations.

For A_2Au^+ cation, isomers 3A and 3B are nearly degenerate in energy. Isomer 3B is higher than isomer 3A by only 0.3 kJ mol^{-1} in energy. Both of them have planar structures with C_s symmetry. The lowest-energy isomer (3A) of A_2Au^+ cation consists of amino-N7H and amino-N9H tautomers of adenine, which are both bound to Au^+ cation through N3 and N1, respectively, similar to the lowest-energy isomer (2A) of AAg^+ cation, but the Au-N bond lengths (2.06 and 2.07 Å) in isomer 3A are shorter than the Ag-N bond lengths (2.17 and 2.16 Å) in isomer 2A. The ∠N—H···N bond angle in isomer 3A is nearly linear (177.2°). Isomer 3B also has the feature of a stronger Au-N bond (2.06 and 2.06 Å) but a weaker hydrogen bond (157.7°). We cannot exclude the existence of isomers 3C–3G in the gas phase since they are slightly higher than isomer 3A in energy.

The BDEs of channels (1a)–(4a) of A_2Au^+ cation are lower than the photon energy of a 266 nm photon, but the BDE of channel (5a) is higher than that of a 266 nm photon, suggesting that the channels (1a)–(4a) for A_2Au^+ cation are possible photodissociation channels at 266 nm. That is also in reasonable agreement with the observation of AAu^+, Au^+, and A^+ fragment ions for the photodissociation of A_2Au^+ cation.

4.2. G_2Cu^+, G_2Ag^+, and G_2Au^+

We note that the structures of the lowest-lying isomers of G_2Cu^+, G_2Ag^+ and G_2Au^+ (4A, 5A and 6A) are almost the same (Fig. 6). They all consist of K-N9H tautomer of guanine, which are both bound to metal ion through N7. The Cu-N bond lengths (1.92 Å and 1.92 Å) are shorter than the Ag-N (2.18 Å and 2.18 Å) and Au-N (2.05 Å and 2.05 Å) bond lengths most likely due to the smaller ionic radius of Cu^+ cation. The second isomer of G_2Cu^+ (4B) is higher in energy than the most stable one (4A) by only 8.8 kJ mol^{-1}. The second isomer of G_2Ag^+ (5B) is higher in energy than 5A by only 10.0 kJ mol^{-1}. Similarly, the second isomer of G_2Au^+ (6B) is higher in energy than 6A by only 9.1 kJ mol^{-1}. The N—H···O bond distances of isomers 4B, 5B and 6B are 1.95, 2.01 and 2.09 Å, respectively. Their bond angles are 171.7°, 171.5° and 164.4°, respectively. According to the previous reported values [66], these bonds can be classified as intermediate hydrogen bonds. Isomers 4C and 4D of G_2Cu^+ cation are much higher than isomer 4A in energy (Fig. 6), so it is unlikely for them to be populated in our experiments. Also, isomers 5C and 5D of G_2Ag^+ cation are much less stable than isomer 5A since their energies are much higher than that of isomer 5A. The same is true for isomers 6C and 6D of GAu^+ cations. Thus, we suggest isomers 4A and 4B, 5A and 5B, 6A and 6 B to be the major products in our experiments. Different from the co-existence of multiple isomers for A_2M^+ (M = Cu, Ag, Au), there are less isomers co-existing for G_2M^+ (M = Cu, Ag, Au).

As can be seen in Table 2, the BDE of channel (1g) of isomer 4A is calculated to be 2.15 eV at the DFT/B3LYP level, much lower than the photon energy of a 266 nm photon. The BDEs of channels (2g), (3g), (4g), and (5g) are calculated to be 5.20, 5.46, 5.33 and 5.58 eV,

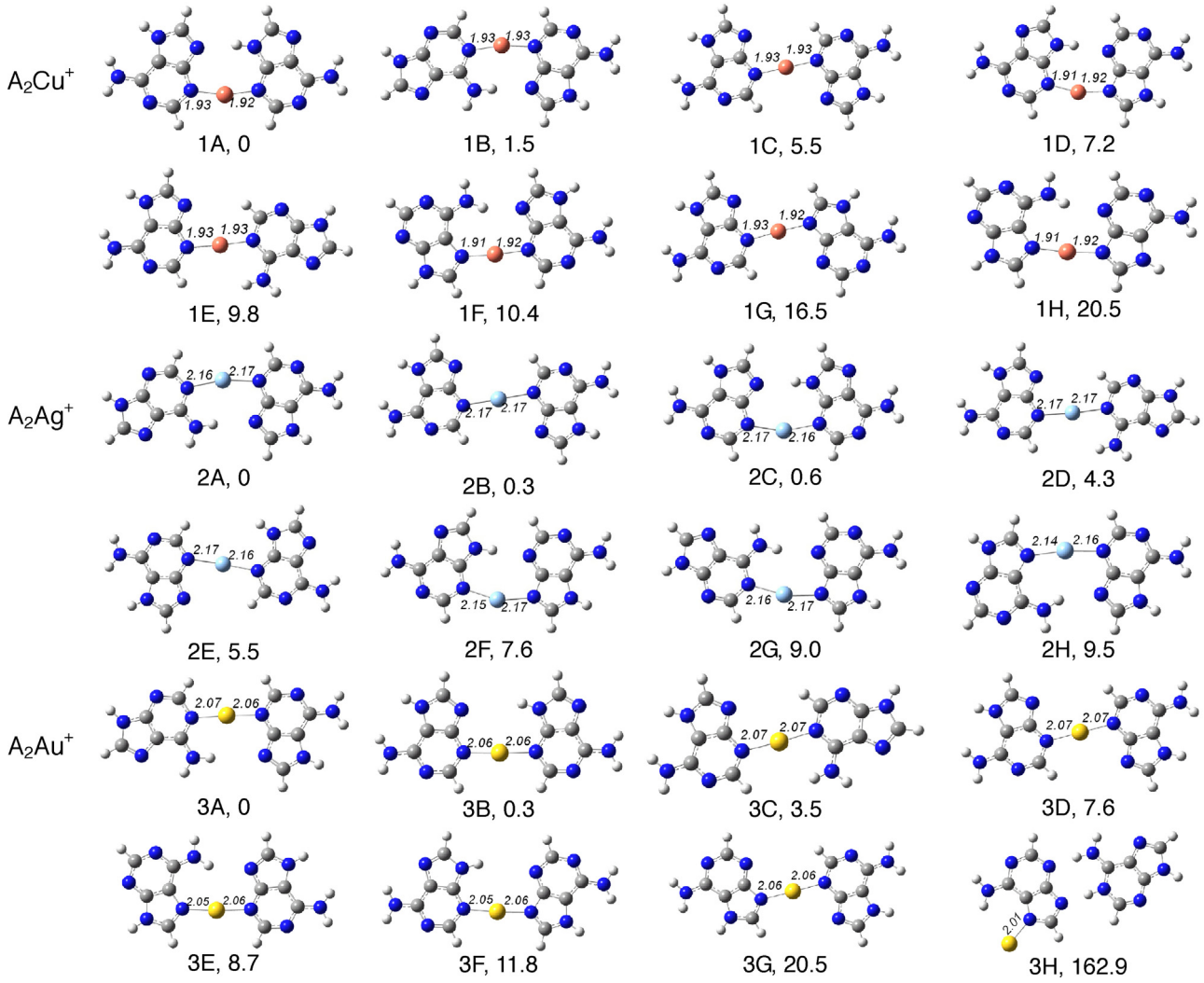

Fig. 5. Low-lying structures of A_2M^+ (M = Cu, Ag, and Au) cations. Their relative energies are shown in kJ mol^{-1}. The M–N bond lengths labeled in the structures are in angstroms.

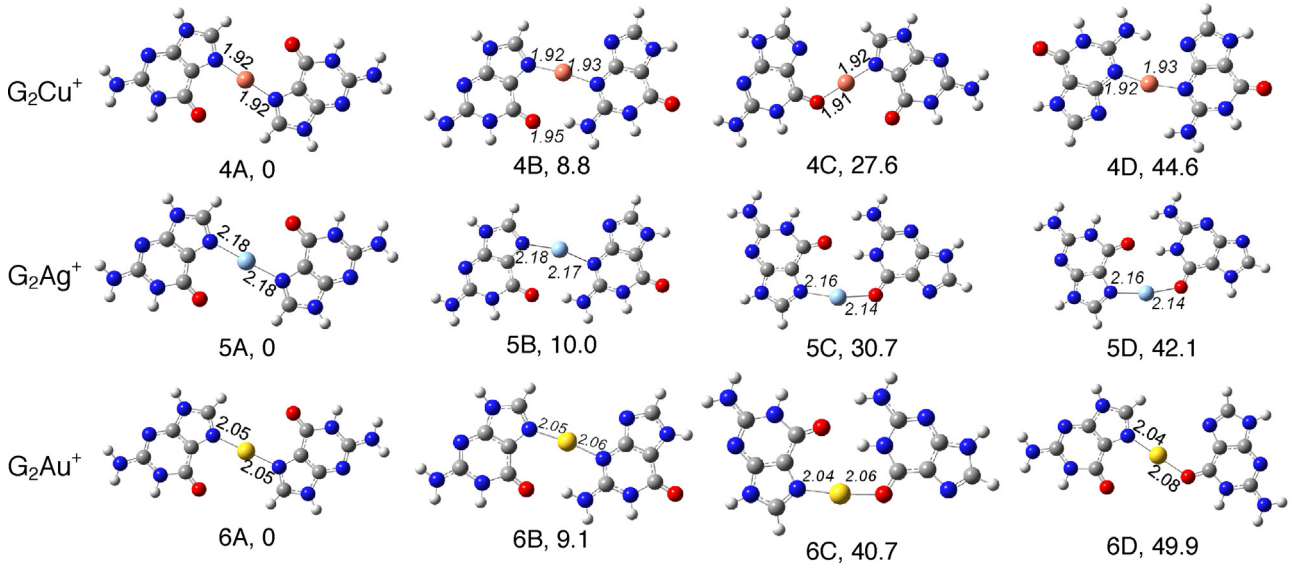

Fig. 6. Low-lying structures of G_2M^+ (M = Cu, Ag, and Au) cations. Their relative energies are shown in kJ mol^{-1}. The M–N bond lengths labeled in the structures are in angstroms.

respectively, much higher than the photon energy of a 266 nm photon. But the BDE of channel (2g) of isomer 4B is 2.87 eV, lower than the photon energy of a 266 nm photon. That is in good agreement with the observation of GCu^+ (channel (1g)) and G^+ (channel (2g) of isomer 4B) fragment ions in the experiment (Fig. 4). The generation of Cu^+ fragment ion (channel (4g)) requires 5.33 eV, which is higher than the photon energy of a 266 nm photon. That explains why Cu^+ fragment ion has not been observed in our experiment. The BDE of the loss of NH_2 group from GCu^+ cation is 4.55 eV. The second strongest fragment ion corresponding to $(C_5N_4H_3O)Cu^+$ cation may arise from the cleavage of C2-N10 bonds on the basis of $G(N9)Cu^+$ cation.

All the BDEs of channels (1g)–(5g) of G_2Ag^+ cation are lower than the photon energy of a 266 nm photon, indicating that all the channels (1g)–(5g) for G_2Ag^+ cation are probable photodissociation channels at 266 nm, which is in reasonable agreement with the observation of Ag^+, G^+, and GAg^+ fragment ions in the photodissociation experiment. The BDE of the loss of HCN group of GAg^+ cation is 4.43 eV, lower than the energy of a 266 nm photon. A second strongest peak corresponds to $(C_4N_4H_4O)Ag^+$ cation more likely due to the simultaneous ruptures of C5-N7 and C8-N9 bonds of $G(9)Ag^+$ cation.

The BDEs of channels (1g)–(3g) of G_2Au^+ cation are 2.62, 4.27, and 4.26 eV, respectively, lower than the photon energy of a 266 nm photon, but the BDEs of channels (4g) and (5g) are 5.79 and 6.04 eV, much higher than the energy of a 266 nm photon, suggesting that the channels (1g)–(3g) for G_2Au^+ cation are probable photodissociation channels at 266 nm. That explains why the GAu^+ and G^+ fragment ions can be detected in the photodissociation experiment while the Au^+ fragment ion has not been detected.

5. Conclusions

Coinage metal ion-nucleobases complexes were generated by laser vaporization and analyzed with time-of-flight mass spectrometry. It is found that, compared to adenine, guanine is able to form relatively larger complexes with the metal ions at similar source conditions. The $(nucleobase)_2M^+$ complexes have relatively high intensities in the mass spectra, indicating that they are very stable. The DFT calculations show that the A_2M^+ and G_2M^+ complexes have planar structures with the metal cations interacting with the N atoms in the carbon-nitrogen rings of adenine and guanine. The A_2M^+ complexes have multiple isomers almost degenerate in energy, while the G_2M^+ complexes each has only two major isomers much lower in energy than the other ones. The dissociation channels depend on the types of nucleobases and metal ions. The photodissociation experiments of A_2M^+ and G_2M^+ complexes at 266 nm show that the loss of one nucleobase (adenine or guanine) molecule is the predominant channel for M = Cu and Ag, while the loss of AAu or GAu are the major channels for M = Au. The Cu^+ fragment ion has not been observed in the photodissociation of A_2Cu^+ and G_2Cu^+ cations because the BDEs of the Cu^+ fragment ion production channels are higher than the energy of a 266 nm photon. For similar reasons, the Au^+ fragment ion has not been detected in the photodissociation of G_2Au^+ cation.

Acknowledgements

This work was supported by the Natural Science Foundation of China (Grant No. 21273246 and 21501114), the Natural Science Foundation of Shanxi Province (Grant No. 2015021048), and the Open Fund of Beijing National Laboratory for Molecular Sciences (Grant No. BNLMS20150051).

Appendix A. Supplementary data

Supplementary data associated with this article can be found, in the online version, at http://dx.doi.org/10.1016/j.ijms.2016.07.008.

References

[1] D. Galaris, A. Evangelou, The role of oxidative stress in mechanisms of metal-induced carcinogenesis, Crit. Rev. Oncol. Hematol. 42 (2002) 93–103.
[2] N. Hadjiliadis, E. Sletten, E. Corporation, Metal Complex–DNA Interactions, Wiley Online Library, 2009.
[3] I. Sissoeff, J. Grisvard, E. Guille, Studies on metal ions–DNA interactions: specific behaviour of reiterative DNA sequences, Prog. Biophys. Mol. Biol. 31 (1976) 165–199.
[4] D.B. Hall, R.E. Holmlin, J.K. Barton, Oxidative DNA damage through long-range electron transfer, Nature 382 (1996) 731–735.
[5] R.B. Martin, Nucleoside sites for transition metal ion binding, Acc. Chem. Res. 18 (1985) 32–38.
[6] H. Sigel, Interactions of metal ions with nucleotides and nucleic acids and their constituents, Chem. Soc. Rev. 22 (1993) 255–267.
[7] S.-i. Nakano, M. Fujimoto, H. Hara, N. Sugimoto, Nucleic acid duplex stability: influence of base composition on cation effects, Nucleic Acids Res. 27 (1999) 2957–2965.
[8] Joseph Shack, R.J. Jenkins, J.M. Thompsett, The interaction of ions and desoxypentose nucleic acid of calf thymus, J. Biol. Chem. 203 (1953) 373–387.
[9] G.L. Eichhorn, Y.A. Shin, Interaction of metal ions with polynucleotides and related compounds. XII. The relative effect of various metal ions on DNA helicity, J. Am. Chem. Soc. 90 (1968) 7323–7328.
[10] G.L. Eichhorn, Metal ions as stabilizers or destabilizers of the deoxyribonucleic acid structure, Nature 194 (1962) 474–475.
[11] W.F. Dove, N. Davidson, Cation effects on the denaturation of DNA, J. Mol. Biol. 5 (1962) 467–478.
[12] D. Yang, A.H.J. Wang, Structural studies of interactions between anticancer platinum drugs and DNA, Prog. Biophys. Mol. Biol. 66 (1996) 81–111.
[13] S.J. Stohs, D. Bagchi, Oxidative mechanisms in the toxicity of metal ions, Free Radic. Biol. Med. 18 (1995) 321–336.
[14] K. Yamamoto, S. Kawanishi, Hydroxyl free radical is not the main active species in site-specific DNA damage induced by copper (II) ion and hydrogen peroxide, J. Biol. Chem. 264 (1989) 15435–15440.
[15] J.L. Sagripant, K.H. Kraemer, Site-specific oxidative DNA damage at polyguanosines produced by copper plus hydrogen peroxide, J. Biol. Chem. 264 (1989) 1729–1734.
[16] V.I. Danilov, V.M. Anisimov, N. Kurita, D. Hovorun, MP2 and DFT studies of the DNA rare base pairs: the molecular mechanism of the spontaneous substitution mutations conditioned by tautomerism of bases, Chem. Phys. Lett. 412 (2005) 285–293.
[17] J.V. Burda, J. Sponer, J. Leszczynski, P. Hobza, Interaction of DNA base pairs with various metal cations (Mg^{2+}, Ca^{2+}, Sr^{2+}, Ba^{2+}, Cu^+, Ag^+, Au^+, Zn^{2+}, Cd^{2+}, and Hg^{2+}): nonempirical ab initio calculations on structures, energies, and nonadditivity of the interaction, J. Phys. Chem. B 101 (1997) 9670–9677.
[18] J. Sponer, M. Sabat, J.V. Burda, J. Leszczynski, P. Hobza, Interaction of the adenine-thymine Watson–Crick and adenine–adenine reverse-Hoogsteen DNA base pairs with hydrated group IIa (Mg^{2+}, Ca^{2+}, Sr^{2+}, Ba^{2+}) and IIb (Zn^{2+}, Cd^{2+}, Hg^{2+}) metal cations: absence of the base pair stabilization by metal-induced polarization effects, J. Phys. Chem. B 103 (1999) 2528–2534.
[19] J.M. Weber, J.A. Kelley, W.H. Robertson, M.A. Johnson, Hydration of a structured excess charge distribution: infrared spectroscopy of the $O_2^-(H_2O)_n$ ($1 <= n <= 5$) clusters, J. Chem. Phys. 114 (2001) 2698–2706.
[20] M.D. Topal, J.R. Fresco, Complementary base pairing and the origin of substitution mutations, Nature 263 (1976) 285–289.
[21] J. Florián, J. Leszczyński, Spontaneous DNA mutations induced by proton transfer in the guanine·cytosine base pairs: an energetic perspective, J. Am. Chem. Soc. 118 (1996) 3010–3017.
[22] L.J.K. Boerner, J.M. Zaleski, Metal complex–DNA interactions: from transcription inhibition to photoactivated cleavage, Curr. Opin. Chem. Biol. 9 (2005) 135–144.
[23] N. Russo, M. Toscano, A. Grand, Bond energies and attachments sites of sodium and potassium cations to DNA and RNA nucleic acid bases in the gas phase, J. Am. Chem. Soc. 123 (2001) 10272–10279.
[24] J. Valdespino-Saenz, A. Martinez, Theoretical study of neutral, anionic, and cationic uracil-Ag and uracil-Au systems: nonconventional hydrogen bonds, J. Phys. Chem. A 112 (2008) 2408–2414.
[25] M.-V. Vazquez, A. Martinez, Theoretical study of cytosine-Al, cytosine-Cu and cytosine-Ag (neutral anionic and cationic), J. Phys. Chem. A 112 (2008) 1033–1039.
[26] A. Martinez, Theoretical study of guanine-Cu and uracil-Cu (neutral anionic, and cationic). Is it possible to carry out a photoelectron spectroscopy experiment? J. Chem. Phys. 123 (2005) 024311–024319.
[27] V. Soto-Verdugo, H. Metiu, E. Gwinn, The properties of small Ag clusters bound to DNA bases, J. Chem. Phys. 132 (2010) 195102–195110.
[28] E.S. Kryachko, F. Remacle, Complexes of DNA bases and gold clusters Au_3 and Au_4 involving nonconventional N–H..Au hydrogen bonding, Nano Lett. 5 (2005) 735–739.

[29] A. Martinez, Do anionic gold clusters modify conventional hydrogen bonds? The interaction of anionic Au-n (n = 2–4) with the adenine-uracil base pair, J. Phys. Chem. A 113 (2009) 1134–1140.
[30] E. Rincon, M. Yanez, A. Toro-Labbe, O. Mo, Effect of Ni (II), Cu (II) and Zn (II) association on the keto-enol tautomerism of thymine in the gas phasewz, Phys. Chem. Chem. Phys. 9 (2007) 2531–2537.
[31] J. Šponer, M. Sabat, J.V. Burda, J. Leszczynski, Metal ions in non-complementary DNA base pairs: an ab initio study of Cu(I), Ag(I), and Au(I) complexes with the cytosine-adenine base pair, J. Biol. Inorg. Chem. 4 (1999) 537–545.
[32] J. Šponer, J.E. Šponer, L. Gorb, J. Leszczynski, B. Lippert, Metal-stabilized rare tautomers and mispairs of DNA bases: N6-metalated adenine and N4-metalated cytosine, theoretical and experimental views, J. Phys. Chem. A 103 (1999) 11406–11413.
[33] J. Anastassopoulou, Metal–DNA interactions, J. Mol. Struct. 651–653 (2003) 19–26.
[34] N. Russo, M. Toscano, A. Grand, Gas-phase theoretical prediction of the metal affinity of copper(I) ion for DNA and RNA bases, J. Mass Spectrom. 38 (2003) 265–270.
[35] L.A. Espinosa Leal, O. Lopez-Acevedo, On the interaction between gold and silver metal atoms and DNA/RNA nucleobases—a comprehensive computational study of ground state properties, Nanotechnol. Rev. 4 (2015) 173–191.
[36] S.A. Krasnokutski, J.S. Lee, D.-S. Yang, High-resolution electron spectroscopy and structures of lithium-nucleobase (adenine uracil, and thymine) complexes, J. Chem. Phys. 132 (2010) 044304–044308.
[37] M.T. Rodgers, P.B. Armentrout, Influence of d orbital occupation on the binding of metal ions to adenine, J. Am. Chem. Soc. 124 (2002) 2678–2691.
[38] H. Liu, J.-L. Sun, Y. Hu, K.-L. Han, S. Yang, Photodissociation of gaseous metal ion-nucleobase complexes: Mg^+-uracil and Mg+-thymine, Chem. Phys. Lett. 389 (2004) 342–347.
[39] J.-L. Sun, H. Liu, H.-M. Wang, K.-L. Han, S. Yang, Photo-induced reactions in the gaseous metal ion-nucleobase complex Mg^+-cytosine, Chem. Phys. Lett. 392 (2004) 285–290.
[40] K. Rajabi, E.A.L. Gillis, T.D. Fridgen, Structures of alkali metal ion-adenine complexes and hydrated complexes by IRMPD spectroscopy and electronic structure calculations, J. Phys. Chem. A 114 (2010) 3449–3456.
[41] C. Fraschetti, M. Montagna, L. Guarcini, L. Guidoni, A. Filippi, Spectroscopic evidence for a gas-phase librating G-quartet–Na+ complex, Chem. Commun. 50 (2014) 14767–14770.
[42] M. Azargun, T.D. Fridgen, Guanine tetrads: an IRMPD spectroscopy, energy resolved SORI-CID, and computational study of M (9-ethylguanine)$_4^+$(M = Li, Na, K, Rb, Cs) in the gas phase, Phys. Chem. Chem. Phys. 17 (2015) 25778–25785.
[43] X. Li, Y.-J. Ko, H. Wang, K.H. Bowen, A. Guevara-Garcia, A. Martinez, Photoelectron and computational studies of the copper-nucleoside anionic complexes, Cu^-(cytidine) and Cu^-(uridine), J. Chem. Phys. 134 (2011) 054315–054318.
[44] G.-J. Cao, H.-G. Xu, R.-Z. Li, W.-J. Zheng, Hydrogen bonds in the nucleobase-gold complexes: photoelectron spectroscopy and density functional calculations, J. Chem. Phys. 136 (2012) 014305.
[45] G.-J. Cao, H.-G. Xu, W.-J. Zheng, J. Li, Theoretical and experimental studies of the interactions between Au_2^- and nucleobases, Phys. Chem. Chem. Phys. 16 (2014) 2928–2935.
[46] J. Gao, G. Berden, M. Rodgers, J. Oomens, Interaction of Cu^+ with cytosine and formation of i-motif-like C–M^+–C complexes: alkali versus coinage metals, Phys. Chem. Chem. Phys. 18 (2016) 7269–7277.
[47] Y.-C. Zhao, Z.-G. Zhang, J.-Y. Yuan, H.-G. Xu, W.-J. Zheng, Modification of reflectron time-of-flight mass spectrometer for photodissociation of mass-selected cluster ions, Chin. J. Chem. Phys. 22 (2009) 655.
[48] S.N. Georgiades, N.H. Abd Karim, K. Suntharalingam, R. Vilar, Interaction of metal complexes with G-quadruplex DNA, Angew. Chem. Int. Ed. 49 (2010) 4020–4034.
[49] C. Lee, W. Yang, R.G. Parr, Development of the Colle-Salvetti correlation-energy formula into a functional of the electron density, Phys. Rev. B 37 (1988) 785.
[50] A.D. Becke, Density-functional thermochemistry. III. The role of exact exchange, J. Chem. Phys. 98 (1993) 5648–5652.
[51] D. Figgen, G. Rauhut, M. Dolg, H. Stoll, Energy-consistent pseudopotentials for group 11 and 12 atoms: adjustment to multi-configuration Dirac–Hartree–Fock data, Chem. Phys. 311 (2005) 227–244.
[52] K.A. Peterson, C. Puzzarini, Systematically convergent basis sets for transition metals. II. Pseudopotential-based correlation consistent basis sets for the group 11 (Cu, Ag Au) and 12 (Zn, Cd, Hg) elements, Theor. Chem. Acc. 114 (2005) 283–296.
[53] G.-J. Cao, W.-J. Zheng, Structures stabilities, and physicochemical properties of nucleobase tautomers, Acta Phys. Chim. Sin. 29 (2013) 2135–2147.
[54] R. Bauernschmitt, R. Ahlrichs, Treatment of electronic excitations within the adiabatic approximation of time dependent density functional theory, Chem. Phys. Lett. 256 (1996) 454–464.
[55] M. Rahman, E. Krishnakumar, Communication: electron ionization of DNA bases, J. Chem. Phys. 144 (2016) 161102.
[56] M.J. Nowak, L. Lapinski, J.S. Kwiatkowski, J. Leszczynski, Molecular structure and infrared spectra of adenine. Experimental matrix isolation and density functional theory study of adenine 15N isotopomers, J. Phys. Chem. 100 (1996) 3527–3534.
[57] K. Rajabi, K. Theel, E.A.L. Gillis, G. Beran, T.D. Fridgen, The structure of the protonated adenine dimer by infrared multiple photon dissociation spectroscopy and electronic structure calculations, J. Phys. Chem. A 113 (2009) 8099–8107.
[58] E. Nir, L. Grace, B. Brauer, M.S. de Vries, REMPI spectroscopy of jet-cooled guanine, J. Am. Chem. Soc. 121 (1999) 4896–4897.
[59] E. Nir, C. Janzen, P. Imhof, K. Kleinermanns, M.S. de Vries, Guanine tautomerism revealed by UV–UV and IR-UV hole burning spectroscopy, J. Chem. Phys. 115 (2001) 4604–4611.
[60] M. Mons, I. Dimicoli, F. Piuzzi, B. Tardivel, M. Elhanine, Tautomerism of the DNA base guanine and its methylated derivatives as studied by gas-phase infrared and ultraviolet spectroscopy, J. Phys. Chem. A 106 (2002) 5088–5094.
[61] M. Mons, F. Piuzzi, I. Dimicoli, L. Gorb, J. Leszczynski, Near-UV resonant two-photon ionization spectroscopy of gas phase guanine: evidence for the observation of three rare tautomers, J. Phys. Chem. A 110 (2006) 10921–10924.
[62] M.Y. Choi, R.E. Miller, Four tautomers of isolated guanine from infrared laser spectroscopy in helium nanodroplets, J. Am. Chem. Soc. 128 (2006) 7320–7328.
[63] E. Nir, C. Janzen, P. Imhof, K. Kleinermanns, M. Vries, Pairing of the nucleobase guanine studied by IR-UV double-resonance spectroscopy and ab initio calculations, Phys. Chem. Chem. Phys. 4 (2002) 740–750.
[64] K. Takahashi, M. Tachikawa, Ab initio post-HF study of guanine dimer isomers involving imino forms in gas phase, J. Mol. Struct. THEOCHEM 912 (2009) 44–52.
[65] M. Berdakin, V. Steinmetz, P. Maitre, G.A. Pino, Gas phase structure of metal mediated (cytosine)$_2Ag^+$ mimics the hemiprotonated (cytosine)$_2H^+$ dimer in i-motif folding, J. Phys. Chem. A 118 (2014) 3804–3809.
[66] B.P. Hay, M. Gutowski, D.A. Dixon, J. Garza, R. Vargas, B.A. Moyer, Structural criteria for the rational design of selective ligands: convergent hydrogen bonding sites for the nitrate anion, J. Am. Chem. Soc. 126 (2004) 7925–7934.